Acta Metallurgica Sinica (English Letters) (2019) 32:677–683
https://doi.org/10.1007/s40195-018-0833-2

High-Speed Friction Stir Welding of SiC_p/Al–Mg–Si–Cu Composite

Chen Wang[1,2] · Bei-Bei Wang[1,2] · Dong Wang[2] · Peng Xue[2] · Quan-Zhao Wang[2] · Bo-Lv Xiao[2] · Li-Qing Chen[1] · Zong-Yi Ma[2]

Received: 3 August 2018 / Revised: 13 September 2018 / Published online: 20 October 2018

Abstract
A 17 vol% SiCp/Al–Mg–Si–Cu composite plate with a thickness of 3 mm was successfully friction stir welded (FSWed) at a very high welding speed of 2000 mm/min for the first time. Microstructural observation indicated that the coarsening of the precipitates was greatly inhibited in the heat-affected zone of the FSW joint at high welding speed, due to the significantly reduced peak temperature and duration at high temperature. Therefore, prominent enhancement of the hardness was achieved at the lowest hardness zone of the FSW joint at this high welding speed, which was similar to that of the nugget zone. Furthermore, the ultimate tensile strength of the joint was as high as 369 MPa, which was much higher than that obtained at low welding speed of 100 mm/min (298 MPa). This study provides an effective method to weld aluminum matrix composite with superior quality and high welding efficiency.

Keywords Friction stir welding · Metal matrix composite · High welding speed · Microstructure · Mechanical property

1 Introduction

Aluminum matrix composite (AMC), as a promising material, has been applied in the aerospace and automotive industries due to the desirable properties including high specific strength, superior wear resistance, low thermal expansion and good stability at elevated temperatures [1]. Usually, welding or joining is an essential processing step during the practical application of AMC. However, according to the investigations by Storjohann et al. [2] and Wang et al. [3], traditional fusion welding brought some drawbacks in the AMC joint, such as large porosity, the incomplete mixing of the parent and filler materials and the formation of deleterious phases.

Friction stir welding (FSW), invented by The Welding Institute (TWI) in 1991, has caught more and more attention in the manufacture area recently, especially when the aluminum alloys were involved [4–7]. At present, FSW has been widely used in various fields, such as aerospace, shipbuilding and railways. As a solid welding technique, FSW should be an effective method of joining AMC, and defect-free joints have been successfully achieved in the previous studies [8–11]. Furthermore, Ni et al. [10] indicate that good tensile and fatigue properties were obtained in a FSW joint of SiCp/2009Al composite. However, most studies focused on investigating the microstructure and properties of the FSW joints at relatively lower welding speeds less than 300 mm/min [8–10], resulting in a low welding efficiency that cannot meet the requirements of industrial manufacture. Generally, a very high welding speed in the range of 1000–2000 mm/min has always been used in FSW of aluminum alloys in the industrial production. Therefore, FSW of AMC at high welding speeds is also an important issue for its practical application.

On the other hand, previous studies by Zhao et al. [12] and Aziz et al. [13] indicate that the strength of the FSW joints can be improved by increasing the welding speed for the precipitation-strengthened aluminum alloys and AMCs. However, the relatively weak flow ability and the serious tool wear during FSW of the AMC inhibited the realization of the high-speed FSW for a long time. Recently, Wang

Available online at http://link.springer.com/journal/40195

✉ Peng Xue
pxue@imr.ac.cn

✉ Bo-Lv Xiao
blxiao@imr.ac.cn

[1] State Key Laboratory of Rolling and Automation, Northeastern University, Shenyang 110819, China

[2] Shenyang National Laboratory for Materials Science, Institute of Metal Research, Chinese Academy of Sciences, Shenyang 110016, China

et al. [14] have successfully performed a high-speed FSW on a SiCp/2009Al-T4 composite with a welding speed of 800 mm/min by using a new cermet tool. Importantly, the ultimate tensile strength (UTS) of the high-speed FSW joint reached up to 97% of the base material (BM). Clearly, increasing the welding speed not only improves the practical welding efficiency, but also provides an effective method to enhance the mechanical properties of the joint.

Then, an interesting question comes: How about the FSW joint of AMC if the welding speed is further increased? In this study, FSW with a very high welding speed of 2000 mm/min was carried out on a SiCp/Al–Mg–Si–Cu composite for the first time, and the microstructure evolution and mechanical properties were investigated subsequently.

2 Experimental Procedures

Rolled plates of 3-mm-thick 17 vol% SiCp/6092Al composite were used in this study. SiC particles had an average size of 2–3 μm, and the chemical composition of the 6092Al alloy was Al–1.0 Mg–0.6Si–0.9Cu (wt%). The received composite was subjected to a T6 treatment (solution at 530 °C for 0.5 h, water quenching and artificial aging at 175 °C for 4 h). The plates were friction stir butt welded along the rolling direction at a tool rotation rate of 2000 rpm and welding speeds of 100, 1000 and 2000 mm/min, which were denoted as FSW-100, FSW-1000 and FSW-2000, respectively. A new TiC-based cermet tool with a shoulder 14 mm in diameter and a threaded conical pin 5 mm in diameter and 2.8 mm in length was used. During FSW, the temperature history in the heat-affected zone (HAZ) was measured by a thermocouple, and the exact measuring site was located at the lowest hardness zone of the joint which was confirmed by the hardness distribution.

The microstructure was examined using optical microscopy (OM) and transmission electron microscopy (TEM). The OM specimens were machined perpendicularly to the welding direction, and subsequently experienced grinding, polishing and etching with a Keller's reagent (190 ml water, 2 ml hydrofluoric acid, 3 ml hydrochloric acid and 5 ml nitric acid). The thin foils for TEM observation, 3 mm in diameter, were prepared by ion-milling technique.

The Vickers hardness profiles of the joints were measured at an interval of 1 mm along the mid-thickness of the welded plate using an automatic testing machine under a load of 500 g for 15 s. The temperature profiles in the heat-affected zones (HAZs) were recorded by embedding the thermocouples in the HAZs during FSW experiments. Tensile specimens with a gauge length of 40 mm and a gauge width of 10 mm were machined perpendicular to the welding direction with the nugget zone (NZ) being in the center of the gauge. Tensile tests were conducted at room temperature with an initial strain rate of 1×10^{-3} s^{-1}.

3 Results and Discussion

The surface morphologies of FSW specimens are shown in Fig. 1. The weld surface of FSW-100 sample seems to be rougher, while FSW-1000 and FSW-2000 samples have relatively clean and smooth surfaces. At a low welding speed, sticky situation was dominant on the contact surface between the tool and workpiece under the shoulder due to the high heat input, leading to the rough surface of the FSW-100 sample [15, 16], whereas the weld surface quality was improved as the heat input decreased, and almost no sharp edges and thick flashes were observed from the weld surfaces of FSW-1000 and FSW-2000 samples.

Figure 2 shows the cross-sectional macrostructures of the FSW joints. It is obvious that defect-free FSW joints

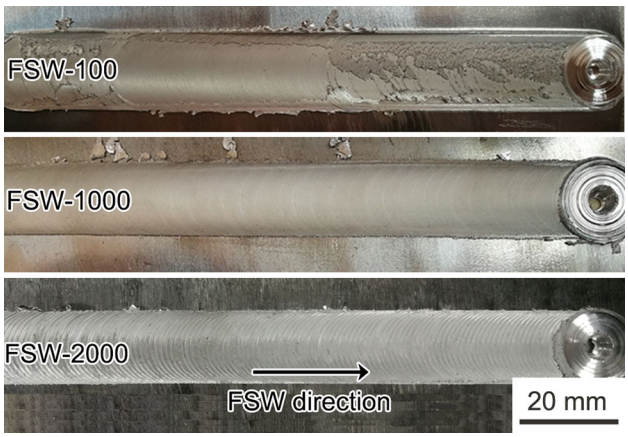

Fig. 1 Surface morphologies of FSW joints at different welding speeds

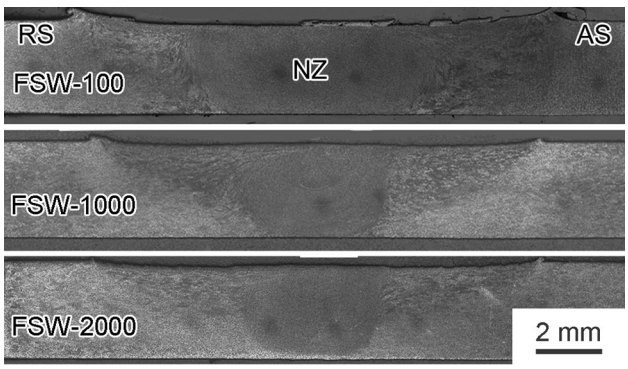

Fig. 2 Cross-sectional macrostructures of the FSW SiCp/6092Al joints

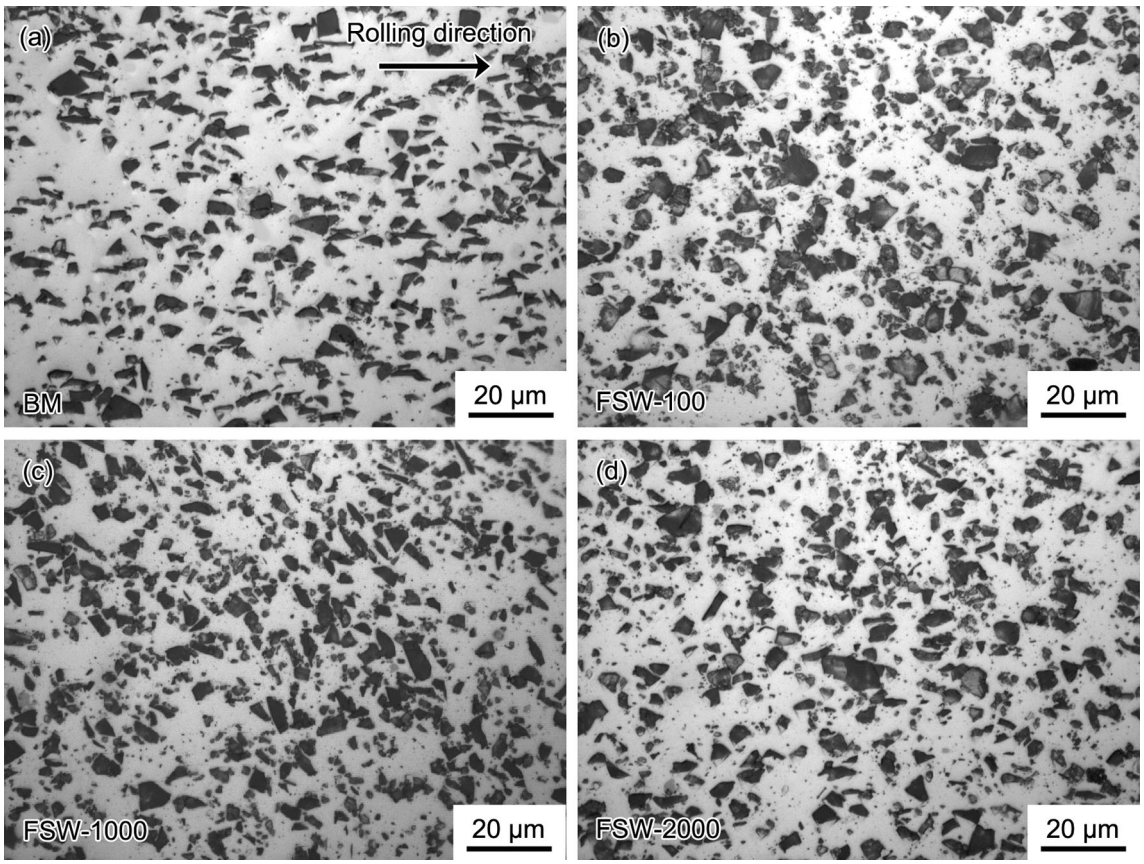

Fig. 3 Optical images of **a** BM and the NZs of FSW SiCp/6092Al joints: **b** FSW-100, **c** FSW-1000, **d** FSW-2000

were obtained from the macrostructures at both low and high welding speeds. The width of the NZ was larger than that of the pin diameter at a low welding speed of 100 mm/min due to the large heat input; however, the width of the NZs reduced clearly at high welding speed of 1000 and 2000 mm/min, which was almost equal to the pin diameter. Obviously, the width of the NZ was closely related to the welding speed during FSW. Similarly, Wang et al. [15] also found that the width of the NZ was reduced as increasing the welding speed in a study on FSW of 6061 Al alloys.

The OM microstructures of the BM and NZs of FSW joints are shown in Fig. 3. In the BM, polygonal SiC particles were homogeneously distributed in the matrix and aligned with the rolling direction (Fig. 3a). The SiC particles were characterized by irregular shape and sharp corners. FSW resulted in the breaking up and redistribution of SiC particles in the NZ of FSW-100 sample (Fig. 3b). In addition, the edges and corners of some SiC particles became blunted and a mass of fine dispersed particles were observed in the NZ. Nevertheless, the SiC particles tended to retain the original morphology and less dispersed particles were observed in the NZs of FSW-1000 and FSW-2000 samples processed at high welding speeds (Fig. 3c, d).

Figure 4 exhibits the hardness profiles of the FSW joints obtained at various welding speeds. It is evident that the softened regions were observed in all the joints. For FSW-100 sample, the hardness distribution exhibited an obvious "W" shape, and two lowest hardness zones (LHZs) with the hardness value of about 84 HV were found in the HAZs on both advancing side (AS) and retreating side (RS),

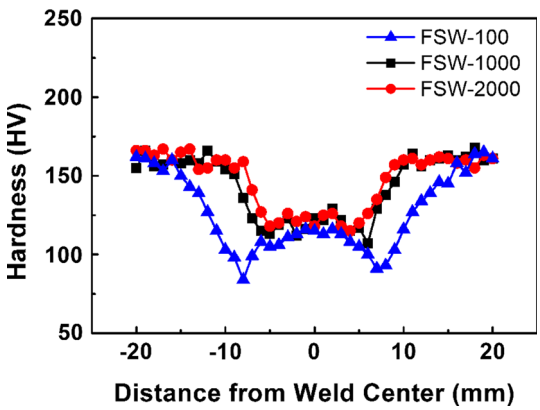

Fig. 4 Hardness profiles of FSW SiCp/6092Al joints

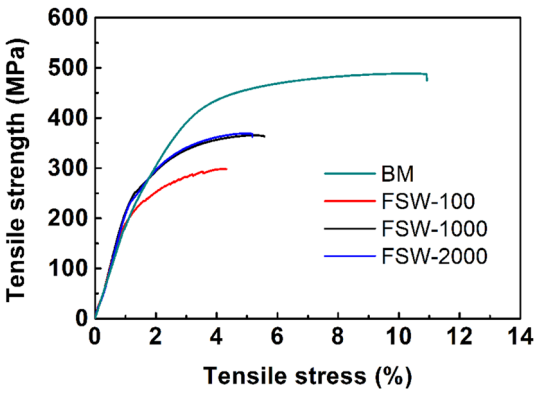

Fig. 5 Tensile curves of FSW SiCp/6092Al joints

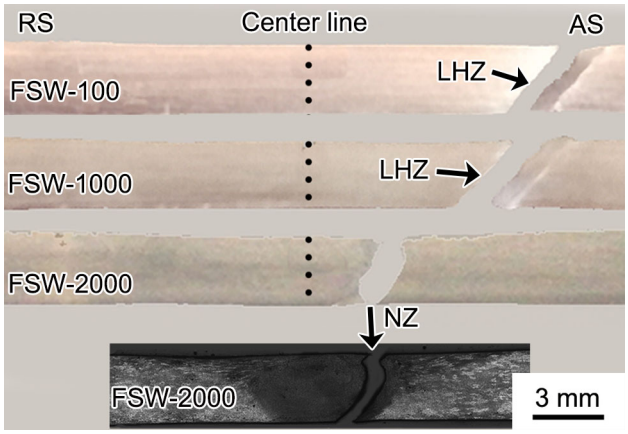

Fig. 6 Fracture locations of FSW SiCp/6092Al joints

similar to that in FSW joints of 6xxx series Al alloys at low welding speeds [15–17]. Compared to the LHZ, obviously enhanced hardness was obtained in the NZ, which reached to about 114 HV.

For FSW-1000 sample, the range of the softened region became narrow and only one obvious LHZ was found at the AS, and the lowest hardness value increased clearly to 107 HV. Furthermore, the hardness value only increased a little to 121 HV in the NZ of FSW-1000 sample compared to that of the FSW-100 sample. While at a very high welding speed of 2000 mm/min, the hardness value in the NZ was similar to that of the FSW-1000 sample, and the lowest hardness value in the LHZ of AS increased to 115 HV for the FSW-2000 sample, which reached to the level of the NZ. Clearly, the hardness could be significantly enhanced at the high welding speed, especially for the lowest hardness value, which plays a crucial role in determining the strength of the FSW joint.

It is clear from the above results that the width of the softening region was obviously reduced and the lowest hardness value was improved as increasing the welding speed, and the same results were also obtained in a FSW joint of 6061 Al alloy by Liu et al. [18]. Moreover, Zhang et al. [19] found the similar phenomenon in FSW of 2219 Al alloys by using the water cooling, which can also greatly reduce the heat input during FSW. Therefore, the heat input can influence the width of the softening region and the lowest hardness value of the FSW joint, which decides the mechanical properties of the whole joint. Then, improving the welding speed and using the water cooling are both effective method to enhance the mechanical properties of the FSW joints by reducing the heat input during FSW.

Figure 5 shows the engineering stress–strain curves of the BM and FSW joints, and the tensile properties are listed in Table 1. The BM exhibited a high UTS of 490 MPa and an elongation of 8%, while the UTS was obviously dropped to 298 MPa for the FSW-100 sample, which was only 60.8% of that of the BM. However, the UTS increased significantly for the FSW joints at high welding speeds of 1000 and 2000 mm/min. Especially, the welding coefficient of FSW-2000 sample reached 75.3%, which was much higher than that of FSW-100 sample and the previous results of FSW AMC joints with 6xxx series Al alloy matrix ($\sim$ 60%) [15–20].

Although the tensile strength of the joint is closely related to the hardness value, the fracture location was not always in accord with the hardness distribution. Figure 6 shows the fracture locations of the tensile specimens at different welding speeds. The fracture locations of FSW-100 and FSW-1000 samples were both along the LHZs,

Table 1 Tensile properties of FSW SiCp/6092Al joints and thermal cycle in the LHZs

Sample	YS (MPa)	UTS (MPa)	El (%)	Welding coefficient (%)	Hardness value in LHZ (HV)	Elevated temperature duration ($\geq$ 100 °C) (s)
FSW-100	190 ± 2	298 ± 2	3.0 ± 0.5	60.8	84	40
FSW-1000	240 ± 4	365 ± 5	4.0 ± 0.5	74.5	107	14
FSW-2000	241 ± 8	369 ± 10	4.0 ± 0.5	75.3	115	9
BM	391 ± 2	490 ± 2	8 ± 0.5	–	163	–

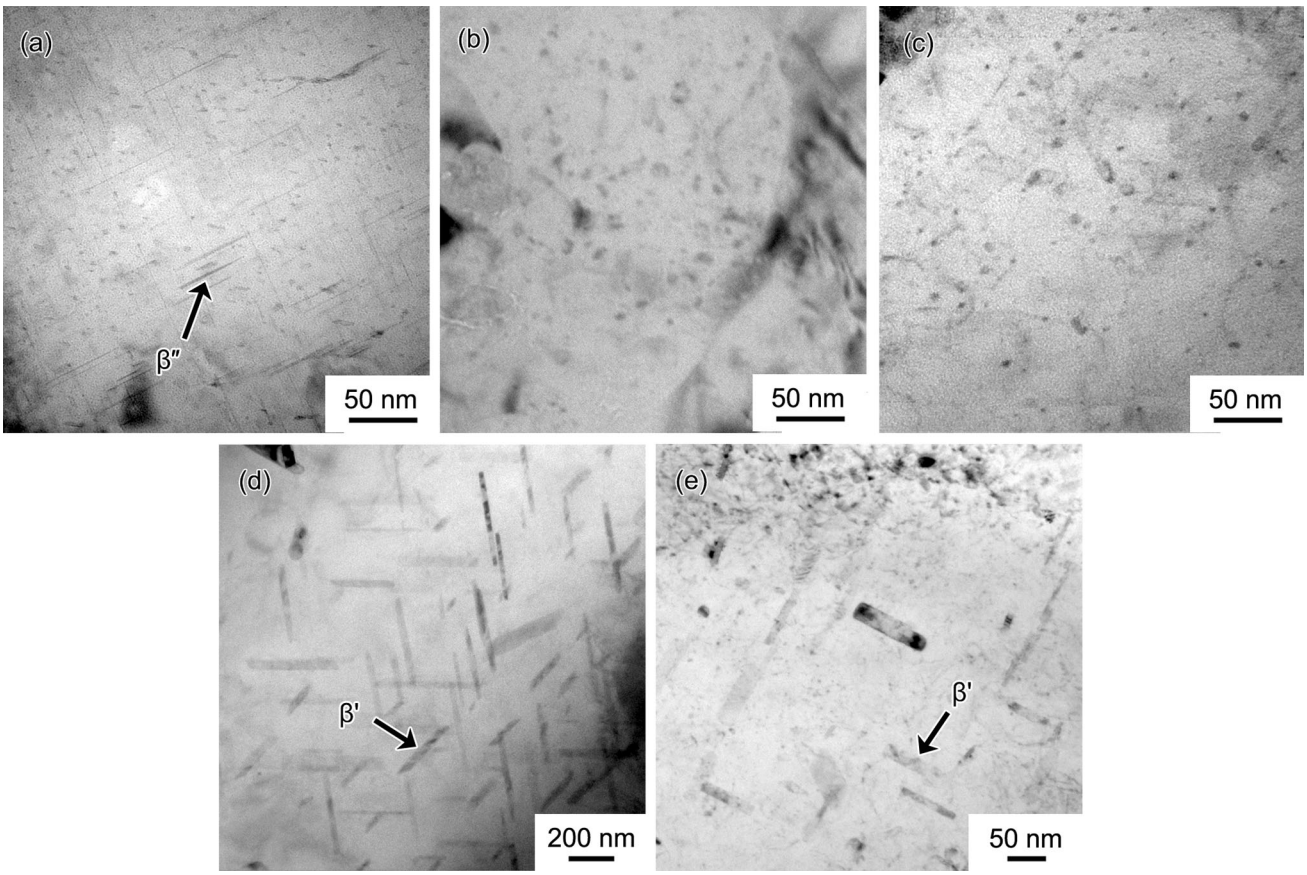

Fig. 7 TEM micrographs of FSW SiCp/6092Al joints: **a** BM, **b** NZ of FSW-100, **c** NZ of FSW-2000, **d** LHZ of FSW-100, **e** LHZ of FSW-2000

whereas FSW-2000 samples fractured at the NZs. According to the previous study by Wang et al. [21], this fracture phenomenon should be related to the difference of the hardness value between the LHZ and NZ. Generally, when the difference of the hardness value between LHZ and NZ was large, such as larger than 15 HV in this study, the fracture preferentially occurred in the LHZ due to the serious softening effect in this zone. However, when the difference of hardness value was small, such as less than 10 HV in this study, the fracture randomly occurred at the NZ of the joint.

Figure 7 reveals the precipitate distribution in the BM and the FSW joints. A high density of needle-shaped precipitates β'' of about 40 nm in length plays essential roles in the strengthening effect of the BM (Fig. 7a). The precipitates dissolved in the Al matrix in the NZs of FSW-100 and FSW-2000 samples, and typical sphere-shaped precipitates were observed in the NZs, as shown in Fig. 7b, c. Such sphere-shaped precipitates were often found after the severe plastic deformation process according to the previous studies [22–24]. Sha et al. [24] suggested that the growth orientation of the precipitates could be changed by the high strain during severe plastic deformation process, and the low-energy interfaces between the precipitates and the Al matrix were lost, resulting in the isotropic growth of the precipitates into a spherical shape. Generally, the strain during FSW process was as high as about 40, and therefore, the formation of sphere-shaped precipitates were reasonable in the NZs according to the investigation by Heurtier et al. [25].

Different from NZ, the HAZ only experienced a thermal cycle, and no plastic deformation occurred in this zone. It is clear that many coarse rod-shaped precipitates β' with the length of about 300 nm were observed in the LHZ (HAZ) of FSW-100 sample (Fig. 7d), suggesting that an overage structure was obtained due to the growth of the needle-shaped β'' precipitates under the thermal cycle. However, the length of the rod-shaped precipitates reduced clearly to about 70 nm in the LHZ of FSW-2000 sample, which were only coarsened slightly compared with those in the BM (Fig. 7e). Zhang et al. [19] also found that the coarsening of the precipitates in the HAZ was inhibited by water cooling in the FSW of 2219 Al alloy, due to the reduced heat input.

The above microstructural evolution of the precipitates in various FSW joints should be related to the thermal cycles during FSW processes. Figure 8 shows the temperature histories recorded at the LHZs of the FSW joints

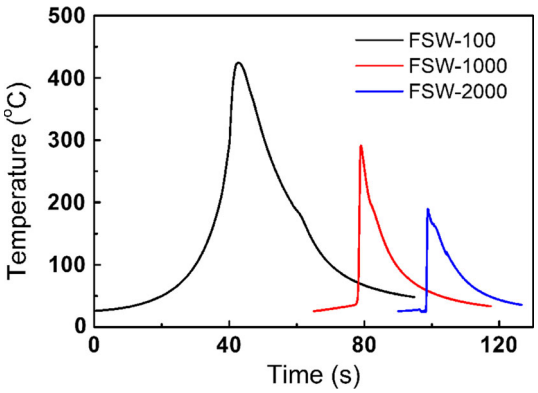

Fig. 8 Temperature histories recorded at LHZs of FSW SiCp/6092Al joints

with different welding speeds, and the specific value was listed in Table 1. Both the peak temperature and elevated temperature (≥ 100 °C) duration in the LHZs reduced as increasing the welding speed. For FSW-100 sample, the peak temperature in the LHZ was about 435 °C. It is reported that the solid solution temperature of the needle-like β'' precipitates in the 6xxx alloys was 220–265 °C [26, 27], so the peak temperature in the LHZ of FSW-100 sample was high enough to dissolve parts of precipitates. On the other hand, the LHZ experienced a long elevated temperature duration of 40 s during FSW, leading to the coarsening of most of β'' precipitates, which were finally changed to the coarsened β' precipitates.

Usually, the thermal cycle in the HAZ can be reduced by decreasing the heat input during FSW process. Wang et al. [28] and Zhang et al. [29] indicated that the peak temperature was reduced and the duration at high temperature was clearly shortened by water cooling in the FSW of Al alloy and steel, respectively. In the case of the high welding speed of 2000 mm/min in this study, the peak temperature in the LHZ was less than 200 °C, and the elevated temperature duration in the LHZ was only 9 s, both of which can effectively inhibit the coarsening effect of β'' precipitates.

For the heat-treatable Al alloys and AMCs, the mechanical properties were mainly associated with the precipitate evolution in the matrix. The softening in the joint can be attributed to the coarsening of β'' precipitates, while the coarsening degree of β'' precipitates was remarkably affected by the thermal cycle. Liu et al. [30] indicated that the welding speed dominated the softening in the LHZ, and the mechanical properties were enhanced with increasing the welding speed. For FSW-100 sample, the LHZ experienced a very long elevated temperature duration during FSW, leading to the coarsening of most of β'' precipitates. In the case of the high welding speed of 2000 mm/min, the elevated temperature duration in the LHZ was greatly reduced, and the coarsening of β'' precipitates was clearly inhibited. Therefore, the significant shortening of the elevated temperature duration was achieved at high welding speed which greatly reduced the coarsening of precipitates, and thus the hardness and strength of the FSW joint were enhanced. Obviously, this study provides an effective method to improve the mechanical properties of the FSW joints for AMCs.

4 Conclusion

In summary, defect-free FSW joints were successfully obtained at a very high welding speed of 2000 mm/min. It was found that the peak temperature decreased clearly and the duration at high temperature during the thermal cycle was greatly shortened in the LHZ of FSW-2000 sample, resulting in the reduced coarsening of the precipitates. Therefore, a high welding coefficient of 75.3% was achieved at a very high welding speed of 2000 mm/min, which was much higher than that at the low welding speed of 100 mm/min (60.8%).

Acknowledgements This work was supported by the National Key R&D Program of China (No. 2017YFB0703104) and National Natural Science Foundation of China (Nos. 51331008 and 51671191).

References

[1] S.C. Tjong, Z.Y. Ma, Mater. Sci. Eng. R **29**, 49 (2000)
[2] D. Storjohann, O.M. Barabash, S.S. Babu, Metall. Mater. Trans. A **36**, 3237 (2005)
[3] X.H. Wang, J.T. Niu, S.K. Guan, L.J. Wang, D.F. Cheng, Mater. Sci. Eng. A **499**, 106 (2009)
[4] G. Liu, L.N. Ma, Z.D. Ma, X.S. Fu, G.B. Wei, Y. Yang, T.C. Xu, W.D. Xie, X.D. Peng, Acta Metall. Sin. (Engl. Lett.) **31**, 853 (2018)
[5] G.Q. Wang, Y.H. Zhao, Y.F. Hao, J. Mater. Sci. Technol. **34**, 73 (2018)
[6] L.H. Wu, K. Nagatsuka, K. Nakata, J. Mater. Sci. Technol. (2018) https://doi.org/10.1016/j.jmst.2018.04.015
[7] P. Xue, D.R. Ni, D. Wang, B.L. Xiao, Z.Y. Ma, Mater. Sci. Eng. A **528**, 4683 (2011)
[8] D.R. Ni, D.L. Chen, D. Wang, B.L. Xiao, Z.Y. Ma, Mater. Sci. Eng. A **608**, 1 (2014)
[9] K. Kalaiselvan, N. Murugan, Trans. Nonferrous Metals Soc. China **23**, 616–624 (2013)
[10] D.R. Ni, D.L. Chen, B.L. Xiao, D. Wang, Z.Y. Ma, Int. J. Fatigue **55**, 64 (2013)
[11] D. Wang, B.L. Xiao, D.R. Ni, Z.Y. Ma, Acta Metall. Sin. (Engl. Lett.) **27**, 816 (2014)
[12] K. Zhao, Z.Y. Liu, B.L. Xiao, Z.Y. Ma, J. Mater. Sci. Technol. **33**, 1004 (2017)
[13] S.B. Aziz, M.W. Dewan, D.J. Huggett, M.A. Wahab, A.M. Okeil, T.W. Liao, Acta Metall. Sin. (Engl. Lett.) **29**, 869 (2016)
[14] D. Wang, Q.Z. Wang, B.L. Xiao, Z.Y. Ma, Mater. Sci. Eng. A **589**, 271 (2014)

[15] T. Wang, Y. Zou, X.M. Liu, K. Matsuda, Mater. Sci. Eng. A **671**, 7 (2016)
[16] H.J. Liu, J.C. Hou, H. Guo, Mater. Des. **47**, 101 (2013)
[17] X.H. Zeng, P. Xue, D. Wang, D.R. Ni, B.L. Xiao, Z.Y. Ma, Sci. Technol. Weld. Join. **23**, 478 (2018)
[18] H.J. Liu, H. Fujii, M. Maeda, K. Nogi, J. Mater. Sci. Lett. **22**, 1061 (2003)
[19] H.J. Zhang, H.J. Liu, L. Yu, J. Mater. Eng. Perform. **21**, 1182 (2012)
[20] X.G. Chen, M. da Silva, P. Gougeon, L. St-Georges, Mater. Sci. Eng. A **518**, 174 (2009)
[21] B.B. Wang, F.F. Chen, F. Liu, W.G. Wang, P. Xue, Z.Y. Ma, J. Mater. Sci. Technol. **33**, 1009 (2017)
[22] G. Sha, K. Tugcu, X.Z. Liao, P.W. Trimby, M.Y. Murashkin, R.Z. Valiev et al., Acta Mater. **63**, 169 (2014)
[23] V.D. Sitdikov, P.S. Chizhov, M.Y. Murashkin, A.A. Goidenko, R.Z. Valiev, Mater. Charact. **110**, 222 (2015)
[24] G. Sha, Y.B. Wang, X.Z. Liao, Z.C. Duan, S.P. Ringer, T.G. Langdon, Acta Mater. **57**, 3123 (2009)
[25] P. Heurtier, C. Desrayaud, F. Montheillet, Mater. Sci. Forum **396**, 1537 (2002)
[26] O. Frigaard, O. Grong, O.T. Midling, Metall. Mater. Trans. A **32**, 1189 (2001)
[27] Y.S. Sato, H. Kokawa, M. Enomoto, S. Jogan, Metall. Mater. Trans. A **30**, 2429 (1999)
[28] Q.Z. Wang, Z.X. Zhao, Y. Zhao, K. Yan, L. Liu, H. Zhang, Mater. Des. **102**, 91 (2016)
[29] H. Zhang, D. Wang, P. Xue, L.H. Wu, D.R. Ni, B.L. Xiao, Z.Y. Ma, J. Mater. Sci. Technol. **34**, 2183 (2018)
[30] F.C. Liu, Z.Y. Ma, Metall. Mater. Trans. A **39**, 2378 (2008)